

# Measurement of single $\pi^0$ production in neutral current neutrino interactions with water by a 1.3 GeV wide band muon neutrino beam

S.Nakayama,<sup>1</sup> C.Mauger,<sup>2,\*</sup> M.H.Ahn,<sup>3</sup> S.Aoki,<sup>4</sup> Y.Ashie,<sup>1</sup> H.Bhang,<sup>3</sup> S.Boyd,<sup>5,\*</sup> D.Casper,<sup>6</sup> J.H.Choi,<sup>7</sup> S.Fukuda,<sup>1</sup> Y.Fukuda,<sup>8</sup> R.Gran,<sup>5</sup> T.Hara,<sup>4</sup> M.Hasegawa,<sup>9</sup> T.Hasegawa,<sup>10</sup> K.Hayashi,<sup>9</sup> Y.Hayato,<sup>11</sup> J.Hill,<sup>2,\*</sup> A.K.Ichikawa,<sup>11</sup> A.Ikeda,<sup>12</sup> T.Inagaki,<sup>9,\*</sup> T.Ishida,<sup>11</sup> T.Ishii,<sup>11</sup> M.Ishitsuka,<sup>1</sup> Y.Itow,<sup>1</sup> T.Iwashita,<sup>11</sup> H.I.Jang,<sup>7,\*</sup> J.S.Jang,<sup>7</sup> E.J.Jeon,<sup>3</sup> K.K.Joo,<sup>3</sup> C.K.Jung,<sup>2</sup> T.Kajita,<sup>1</sup> J.Kameda,<sup>1</sup> K.Kaneyuki,<sup>1</sup> I.Kato,<sup>9</sup> E.Kearns,<sup>13</sup> A.Kibayashi,<sup>14</sup> D.Kielczewska,<sup>15,16</sup> B.J.Kim,<sup>3</sup> C.O.Kim,<sup>17</sup> J.Y.Kim,<sup>7</sup> S.B.Kim,<sup>3</sup> K.Kobayashi,<sup>2</sup> T.Kobayashi,<sup>11</sup> Y.Koshio,<sup>1</sup> W.R.Kropp,<sup>6</sup> J.G.Learned,<sup>14</sup> S.H.Lim,<sup>7</sup> I.T.Lim,<sup>7</sup> H.Maesaka,<sup>9</sup> T.Maruyama,<sup>11,\*</sup> S.Matsuno,<sup>14</sup> C.McGrew,<sup>2</sup> A.Minamino,<sup>1</sup> S.Mine,<sup>6</sup> M.Miura,<sup>1</sup> K.Miyano,<sup>18</sup> T.Morita,<sup>9</sup> S.Moriyama,<sup>1</sup> M.Nakahata,<sup>1</sup> K.Nakamura,<sup>11</sup> I.Nakano,<sup>12</sup> F.Nakata,<sup>4</sup> T.Nakaya,<sup>9</sup> T.Namba,<sup>1</sup> R.Nambu,<sup>1</sup> K.Nishikawa,<sup>9</sup> S.Nishiyama,<sup>4</sup> K.Nitta,<sup>11</sup> S.Noda,<sup>4</sup> Y.Obayashi,<sup>1</sup> A.Okada,<sup>1</sup> Y.Oyama,<sup>11</sup> M.Y.Pac,<sup>19</sup> H.Park,<sup>11,\*</sup> C.Saji,<sup>1</sup> M.Sakuda,<sup>11,\*</sup> A.Sarrat,<sup>2</sup> T.Sasaki,<sup>9</sup> N.Sasao,<sup>9</sup> K.Scholberg,<sup>20</sup> M.Sekiguchi,<sup>4</sup> E.Sharkey,<sup>2</sup> M.Shiozawa,<sup>1</sup> K.K.Shiraishi,<sup>5</sup> M.Smy,<sup>6</sup> H.W.Sobel,<sup>6</sup> J.L.Stone,<sup>13</sup> Y.Suga,<sup>4</sup> L.R.Sulak,<sup>13</sup> A.Suzuki,<sup>4</sup> Y.Suzuki,<sup>1</sup> Y.Takeuchi,<sup>1</sup> N.Tamura,<sup>18</sup> M.Tanaka,<sup>11</sup> Y.Totsuka,<sup>11</sup> S.Ueda,<sup>9</sup> M.R.Vagins,<sup>6</sup> C.W.Walter,<sup>13</sup> W.Wang,<sup>13</sup> R.J.Wilkes,<sup>5</sup> S.Yamada,<sup>1,\*</sup> S.Yamamoto,<sup>9</sup> C.Yanagisawa,<sup>2</sup> H.Yokoyama,<sup>21</sup> J.Yoo,<sup>3</sup> M.Yoshida,<sup>22</sup> and J.Zalipska<sup>16</sup>

(The K2K Collaboration)

<sup>1</sup> Institute for Cosmic Ray Research, University of Tokyo, Kashiwa, Chiba 277-8582, JAPAN

<sup>2</sup> Department of Physics and Astronomy, State University of New York, Stony Brook, NY 11794-3800, USA

<sup>3</sup> Department of Physics, Seoul National University, Seoul 151-742, KOREA

<sup>4</sup> Kobe University, Kobe, Hyogo 657-8501, JAPAN

<sup>5</sup> Department of Physics, University of Washington, Seattle, WA 98195-1560, USA

<sup>6</sup> Department of Physics and Astronomy, University of California, Irvine, Irvine, CA 92697-4575, USA

<sup>7</sup> Department of Physics, Chonnam National University, Kwangju 500-757, KOREA

<sup>8</sup> Department of Physics, Miyagi University of Education, Sendai 980-0845, JAPAN

<sup>9</sup> Department of Physics, Kyoto University, Kyoto 606-8502, JAPAN

<sup>10</sup> Research Center for Neutrino Science, Tohoku University, Sendai, Miyagi 980-8578, JAPAN

<sup>11</sup> High Energy Accelerator Research Organization (KEK), Tsukuba, Ibaraki 305-0801, JAPAN

<sup>12</sup> Department of Physics, Okayama University, Okayama, Okayama 700-8530, JAPAN

<sup>13</sup> Department of Physics, Boston University, Boston, MA 02215, USA

<sup>14</sup> Department of Physics and Astronomy, University of Hawaii, Honolulu, HI 96822, USA

<sup>15</sup> Institute of Experimental Physics, Warsaw University, 00-681 Warsaw, POLAND

<sup>16</sup> A. Soltan Institute for Nuclear Studies, 00-681 Warsaw, POLAND

<sup>17</sup> Department of Physics, Korea University, Seoul 136-701, KOREA

<sup>18</sup> Department of Physics, Niigata University, Niigata, Niigata 950-2181, JAPAN

<sup>19</sup> Department of Physics, Dongshin University, Naju 520-714, KOREA

<sup>20</sup> Department of Physics, Massachusetts Institute of Technology, Cambridge, MA 02139, USA

<sup>21</sup> Department of Physics, Tokyo University of Science, Noda, Chiba 278-0022, JAPAN

<sup>22</sup> Department of Physics, Osaka University, Toyonaka, Osaka 560-0043, JAPAN

(Dated: August 14, 2004)

Neutral current single  $\pi^0$  production induced by neutrinos with a mean energy of 1.3 GeV is measured at a 1000 ton water Cherenkov detector as a near detector of the K2K long baseline neutrino experiment. The cross section for this process relative to the total charged current cross section is measured to be  $0.064 \pm 0.001$  (*stat.*)  $\pm 0.007$  (*sys.*). The momentum distribution of produced  $\pi^0$ s is measured and is found to be in good agreement with an expectation from the present knowledge of the neutrino cross sections.

PACS numbers: 13.15.+g, 14.60.Lm, 25.30.Pt

After the discovery of atmospheric neutrino oscillations by Super-Kamiokande in 1998 [1], the primal aim of current and future long baseline (LBL) experiments using an accelerator-based neutrino beam is more accurate de-

termination of oscillation parameters. The uncertainties on the knowledge of the neutrino-nucleus cross sections and subsequent nuclear effects in the GeV neutrino energy region could become a severe limitation in future oscillation studies. For reducing these systematic uncertainties, near detectors of LBL experiments can provide neutrino interaction data with much higher statistics and better quality than existing data.

A single  $\pi^0$  event is a good signature of neutral current

\*For current affiliations see

<http://neutrino.kek.jp/present-addresses0408.ps>.

(NC) neutrino interactions in the GeV region. Especially in a water Cherenkov detector, a decay of the  $\pi^0$  can be clearly identified as two electromagnetic-showering Cherenkov rings. The single  $\pi^0$  production rate by atmospheric neutrinos could be usable to distinguish between the  $\nu_\mu \leftrightarrow \nu_\tau$  and  $\nu_\mu \leftrightarrow \nu_s$  oscillation hypotheses. The NC rate is attenuated in the case of transitions of  $\nu_\mu$ 's into sterile neutrinos, while it does not change in the  $\nu_\mu \leftrightarrow \nu_\tau$  scenario. An understanding of single  $\pi^0$  production is also very important for a search for electron neutrino appearance in LBL experiments with a water Cherenkov detector, because the most serious background to single-ring  $\nu_e$  signals is a single  $\pi^0$  event with only one ring reconstructed due to highly asymmetric energies or small opening angle of two  $\gamma$ -rays in the  $\pi^0$  decay [2].

These single  $\pi^0$ s in the GeV neutrino energy region are mainly produced via the  $\Delta$  resonance as  $\nu + N \rightarrow \nu + \Delta$ ,  $\Delta \rightarrow N' + \pi^0$ , where  $N$  and  $N'$  are nucleons. Because of nuclear effects such as Fermi motion, Pauli blocking, nuclear potential and final state interactions,  $\Delta$  production and its decay could be different from a simple picture of neutrino-nucleon interactions. In addition, final state interactions of nucleons and mesons during a traversal of nuclear matter could largely modify the number, momenta, directions and charge states of produced particles. Though there exist several theoretical approaches for modeling these processes, their uncertainties are still large. There exist very little experimental data for NC single  $\pi^0$  production and no reports on measurements with a water target, which is the target matter of a far detector in some of the LBL experiments [3, 4]. It is clear that a good knowledge of NC single  $\pi^0$  production cross section and  $\pi^0$  momentum distribution is required for the above studies. In this letter, we present the first high statistics measurement of “NC1 $\pi^0$ ” interactions in water defined as a neutral current neutrino interaction where just a single  $\pi^0$  and no other mesons are emitted in the final state from a nucleus.

The KEK to Kamioka long baseline neutrino oscillation experiment (K2K) uses an almost pure muon neutrino beam (98.2%  $\nu_\mu$ , 1.3%  $\nu_e$  and 0.5%  $\bar{\nu}_\mu$ ) with a mean neutrino energy of 1.3 GeV. This intense wide-band beam is produced by the KEK proton synchrotron (KEK-PS). Protons with 12 GeV kinetic energy extracted from the KEK-PS are bent toward the far detector, Super-Kamiokande, located 250 km away from KEK and interact with an aluminum target. Positively charged secondary particles, mainly  $\pi^+$ 's, are focused with a pair of magnetic horns and then decay to produce a neutrino beam. Figure 1 shows the energy spectrum of the K2K neutrino beam at 300 m downstream from the target in the near site with a  $10^{20}$  protons on target (POT) exposure predicted by a beam simulation [3]. The beam simulation is validated by a pion monitor (PIMON), which measures the momentum and divergence of pions just behind the second horn [3]. The flux shape is also measured through neutrino interactions by K2K near detectors [5].

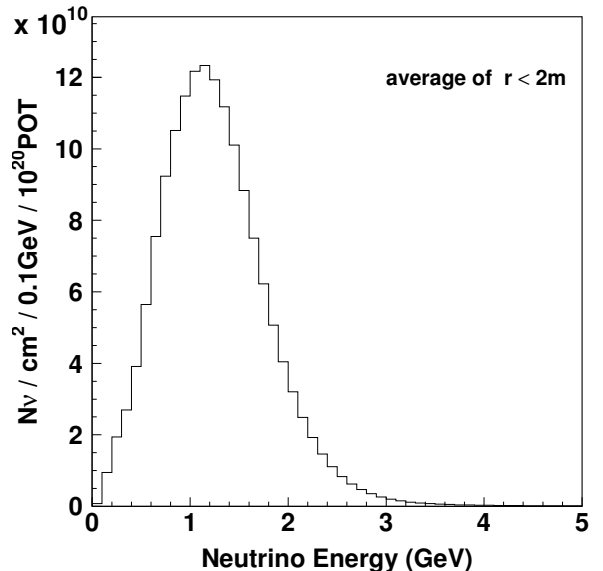


FIG. 1: The energy spectrum of the K2K neutrino beam at 300 m downstream from the target in the near site with a  $10^{20}$  protons on target exposure predicted by a neutrino beam simulation. The spectrum is averaged within 2 m from the beam center.

The absolute flux estimation, however, is not easy due to uncertainties of the primary proton beam absolute intensity, the proton beam profile and the proton targeting efficiency. Instead of deriving the absolute cross section for NC1 $\pi^0$  interactions, we measure the relative NC1 $\pi^0$  cross section to the total charged current (CC) cross section, since the CC is a good experimental signature.

As one of the near detectors for K2K, a 1,000 ton water Cherenkov detector (1kt) is located about 300 m downstream of the pion production target. The 1kt detector is a miniature of Super-Kamiokande using the same interaction target matter and instrumentation. The inner volume of the 1kt detector is a cylinder with 8.6 m diameter and a height of 8.6 m. This volume is viewed by 680 photomultiplier tubes (PMTs) of 50 cm diameter, facing inward to detect Cherenkov light from neutrino events. The PMTs and their arrangement are identical to those of Super-Kamiokande, giving a 40% photocathode coverage. The primal role of the 1kt detector is to measure the  $\nu_\mu$  interaction rate and the  $\nu_\mu$  energy spectrum. The 1kt detector also provides a good measurement of high statistics neutrino-water interactions. The analysis in this letter is based on the 1kt data taken between January 2000 and July 2001, corresponding to  $3.2 \times 10^{19}$  POT.

The data acquisition (DAQ) system of the 1kt detector is also similar to that of Super-Kamiokande. A signal from each PMT is processed by custom electronics modules called ATMs, which are developed for the Super-Kamiokande experiment and are used for recording digitized charge and timing informations of each PMT hit over a threshold of about 1/4 photoelectrons [6]. The DAQ trigger threshold is about 40 hits of PMTs within

a 200 nsec window in a  $1.2 \mu\text{sec}$  beam spill gate, which is roughly equivalent to a signal of a 6 MeV electron. The analog sum of all 680 PMTs' signals (PMTSUM) is also recorded for every beam spill by a 500 MHz FADC to identify multi interactions in a spill gate. We determine the number of interactions in each spill by counting the peaks in PMTSUM greater than a threshold equivalent to a 100 MeV electron signal.

Physical parameters of an event in the 1kt detector such as the vertex position, the number of Cherenkov rings, particle types and momenta are determined by the same algorithms as used in Super-Kamiokande [7, 8]. First, the vertex position of an event is determined by timing information of PMT hits. With knowledge of the vertex position, the number of Cherenkov rings and their directions are determined by a maximum-likelihood procedure. Each ring is then classified as  $e$ -like representing a showering particle ( $e^\pm, \gamma$ ) or  $\mu$ -like representing a non-showering particle ( $\mu^\pm, \pi^\pm$ ) using its ring pattern. On the basis of this particle type information, the vertex position of a single-ring event is further refined. The momentum corresponding to each ring is determined from the intensity of Cherenkov light.

In this analysis, neutrino interaction candidates are selected by the following requirements : (i) An event is triggered within a  $1.2 \mu\text{sec}$  beam spill gate. (ii) There is no detector activity within a  $1.2 \mu\text{sec}$  window preceding a beam spill. (iii) Only a single event is observed by the PMTSUM peak search in that spill. (iv) The reconstructed vertex position is in the 25 ton fiducial volume defined as a 4 m diameter, 2 m long cylinder along the beam axis. (v) The visible energy is larger than 30 MeV. A total of 60,545 events remain after cuts (i) to (v).

Single  $\pi^0$  events are extracted from the sample of fully contained (FC) neutrino events, which deposit all of their Cherenkov light inside the inner detector. An exiting particle deposits a large amount of energy at the PMT of the exiting position. Therefore, the FC events are selected by requiring the maximum number of photoelectrons on a single PMT at the exit direction of the most energetic particle to be less than 200. The events with the maximum number of photoelectrons greater than 200 are identified as a partially contained (PC) event. Because  $\pi^0$ s mostly decay into two  $\gamma$ -rays, the following criteria are further applied to the FC sample in order to select single  $\pi^0$  events : (1) The number of reconstructed rings is two. (2) Both rings have a showering type ( $e$ -like) particle identification. (3) The invariant mass is in the range of  $85 - 215 \text{ MeV}/c^2$ . Figure 2 shows the invariant mass distribution of the events which satisfy cuts (1) and (2). A  $\pi^0$  mass peak is clearly visible. The peaks for both the observed data and the neutrino Monte Carlo events are slightly shifted towards higher values compared to the nominal value of the  $\pi^0$  mass,  $135 \text{ MeV}/c^2$ . This shift is due to a vertex reconstruction bias of a few dozen cm and an energy deposit by de-excitation  $\gamma$ -rays from an oxygen nucleus. The difference in peak position between

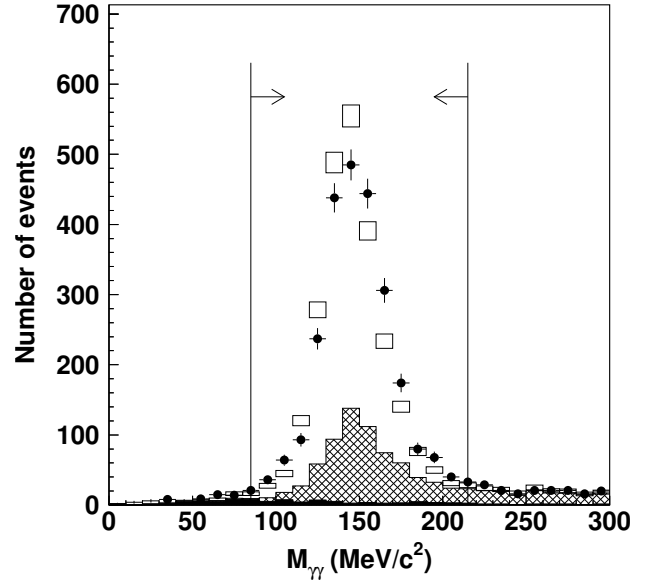


FIG. 2: The invariant mass of two  $e$ -like ring events for the experimental data (black dots) and the neutrino Monte Carlo simulation (box histogram). The Monte Carlo histogram is normalized to the area of the data histogram. The error bars are statistical only. The black portion and the hatched portion in the Monte Carlo histogram show the non- $\pi^0$  component and non-NC1 $\pi^0$  component, respectively. A pair of arrows shows the invariant mass cut (3) (see text).

	Data	NC1 $\pi^0$ efficiency
FC	45317	97 %
Two rings	11117	57 %
Both $e$ -like	3150	48 %
Invariant mass	2496	47 %

TABLE I: The number of events after each selection to make the single  $\pi^0$  sample in 1kt data. The Monte Carlo efficiencies are calculated for NC1 $\pi^0$  interactions whose real vertex is in the fiducial volume.

the data distribution and the Monte Carlo prediction is within our quoted  $^{+2}_{-3}$  % systematic uncertainty for the absolute energy scale. A total of 2,496 single  $\pi^0$  events are collected by these criteria as shown in Table I.

Figure 3-(a) shows the reconstructed  $\pi^0$  momentum distribution for the single  $\pi^0$  sample. The momentum resolution for 200 MeV/ $c$   $\pi^0$ s in NC1 $\pi^0$  events is estimated to be about 15 MeV/ $c$ . The single  $\pi^0$  sample contains a background of non-NC1 $\pi^0$  events shown as a hatched histogram in Figures 2 and 3-(a). The background contamination is estimated by the neutrino Monte Carlo simulation and is subtracted.

The neutrino interactions with water are simulated by the NEUT program library. A detailed description of NEUT can be found in Ref. [9]. Quasi-elastic scattering is simulated based on the Llewellyn Smith's model [10].

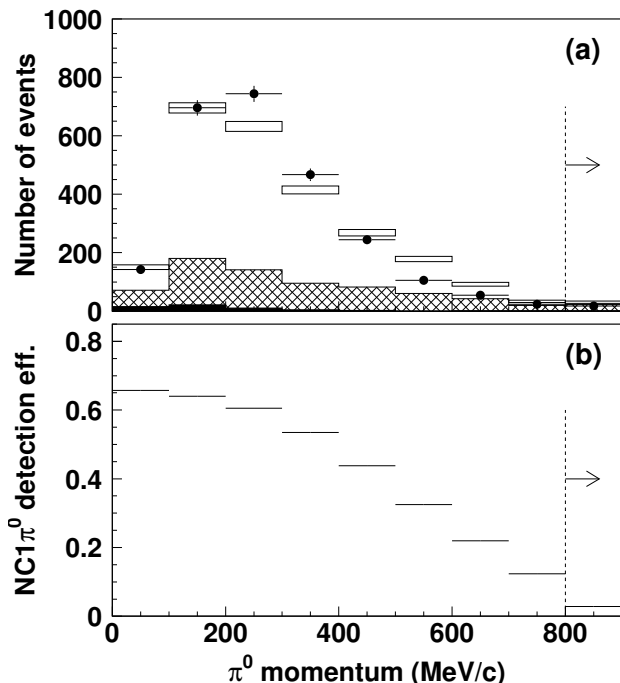


FIG. 3: (a) The reconstructed  $\pi^0$  momentum distribution for the single  $\pi^0$  sample, comparing 1kt data (black dots) and the neutrino Monte Carlo simulation (box histogram). The Monte Carlo histogram is normalized to the area of the data histogram. The error bars are statistical only. The black portion and the hatched portion in the Monte Carlo histogram show the non- $\pi^0$  component and non-NC1 $\pi^0$  component, respectively. (b) The detection efficiency for NC1 $\pi^0$  interactions as a function of real  $\pi^0$  momentum. The highest momentum bin in each figure integrates the events above 800 MeV/c.

The Rein and Sehgal's model [11] is used to simulate single meson production mediated by a baryon resonance. The decay kinematics of the  $\Delta(1232)$  resonance is also determined by the Rein and Sehgal's method. For the decays of the other resonances, the generated mesons are assumed to be emitted isotropically in the resonance rest frame. A twenty percent suppression of pion production is adopted for simulating pion-less  $\Delta$  decay, where the event contains only a lepton and a nucleon in the final state [12]. The axial vector mass,  $M_A$ , is set to 1.1 GeV/ $c^2$  for both the quasi-elastic scattering and the single meson production models. Coherent pion production is simulated using the Rein and Sehgal's model [13] with modified cross section according to a description by Marteau et al. [14]. For deep inelastic scattering, GRV94 nucleon structure function [15] with a correction by Bodek and Yang [16] is used to calculate the cross section. In order to generate the final state hadrons, PYTHIA/JETSET [17] package is used for the hadronic invariant mass,  $W$ , larger than 2.0 GeV/ $c^2$ . A custom-made program [18] is used for  $W$  in the range of 1.3 – 2.0 GeV/ $c^2$ . Nuclear effects for  $\nu$ - $^{16}\text{O}$  scattering are also taken into account. Fermi motion of nucleons is simulated using the relativistic Fermi gas model.

Pauli blocking effect is considered in the simulation of quasi-elastic scattering and single meson production. Pions generated in  $^{16}\text{O}$  are tracked taking into account their inelastic scattering, charge exchange and absorption. The pion generation point in the nucleus is set according to Woods and Saxon's nucleon density distribution [19]. The mean free path of each pion interaction is calculated using the model by Salcedo et al. [20]. The direction and momentum of pions after inelastic scattering or charge exchange are determined based on the results of a phase shift analysis obtained from  $\pi$  -  $N$  scattering experiments [21]. Emission of de-excitation low energy  $\gamma$ -rays from a hole state of residual nuclei is also taken into account [22]. Outside the nucleus, particles are tracked using GEANT and CALOR packages except pions with momenta smaller than 500 MeV/ $c$ , which are tracked with a custom-made program [18] in order to consider the  $\Delta$  resonance correctly.

The NC1 $\pi^0$  fraction in the single  $\pi^0$  sample, predicted by the neutrino Monte Carlo simulation, is estimated to be 71 % (52 % from single  $\pi^0$  production via a resonance decay, 3 % from single  $\pi^\pm$  production via a resonance decay and subsequent charge exchange into  $\pi^0$  in the target nucleus, 10 % from coherent  $\pi^0$  production and 4 % from neutrino deep inelastic scattering where the rest of mesons are absorbed inside the nucleus). The non-NC1 $\pi^0$  background, which accounts for 29 % of the single  $\pi^0$  sample as shown in Figures 2 and 3, contains NC  $\pi^0$  production where outgoing mesons except a single  $\pi^0$  have low momenta (7 %), CC  $\pi^0$  production where accompanying muon and mesons have low momenta (9 %),  $\pi^0$  production by a recoil nucleon or mesons outside the target nucleus (10 %), and non- $\pi^0$  background due to mis-reconstruction (3 %).

The NC1 $\pi^0$  fraction is estimated for each of the ten  $\pi^0$  momentum bins shown in Figure 3-(a). The number of observed single  $\pi^0$  events in each  $\pi^0$  momentum bin is multiplied by the NC1 $\pi^0$  fraction for the corresponding momentum bin. The systematic errors attributed to this background subtraction procedure are estimated by assuming uncertainties in neutrino interaction models as listed in Table II-(A). The  $M_A$  value in the models for quasi-elastic scattering and single meson production is varied by  $\pm 10\%$  from a central value of 1.1 GeV/ $c^2$ . The error due to the uncertainty on coherent pion production cross section is estimated by removing the cross section modification by Marteau et al.. For deep inelastic scattering, the effect of the correction on nucleon structure function according to Bodek and Yang's description is evaluated. The systematic errors due to nuclear effect uncertainties are evaluated by varying the probabilities of pion absorption and inelastic scattering (including charge exchange) in  $^{16}\text{O}$  nucleus independently by  $\pm 30\%$ .

After estimating the number of NC1 $\pi^0$  interactions in each  $\pi^0$  momentum bin, we apply a fiducial volume correction. The number of NC1 $\pi^0$  interactions in the Monte Carlo single  $\pi^0$  sample increases by about 2 % if

Sources	Errors (%)
<b>(A) Systematic uncertainties in background subtraction</b>	
$M_A$ in quasi-elastic and single meson ( $\pm 10\%$ )	0.2
Quasi-elastic scattering (total cross section, $\pm 10\%$ )	0.0
Single meson production (total cross section, $\pm 10\%$ )	0.9
Coherent pion production (model dependence)	1.6
Deep inelastic scattering (model dependence)	5.1
Deep inelastic scattering (total cross section, $\pm 5\%$ )	0.5
NC/CC ratio ( $\pm 20\%$ )	3.2
Nuclear effects for pions in $^{16}\text{O}$ (absorption, $\pm 30\%$ )	1.5
Nuclear effects for pions in $^{16}\text{O}$ (inelastic scattering, $\pm 30\%$ )	0.7
Pion production outside the target nucleus (total cross section, $\pm 20\%$ )	2.3
<b>(B) Systematic uncertainties in fiducial volume correction</b>	
Fiducial cut	1.6
<b>(C) Systematic uncertainties in efficiency correction</b>	
Ring counting	5.4
Particle identification	4.2
Energy scale	0.3

TABLE II: Summary of the systematic errors on the measurement of the number of  $\text{NC}1\pi^0$  interactions.

real vertices are used instead of reconstructed vertices in the fiducial volume selection. The data are then multiplied by 1.02 in order to derive the number of  $\text{NC}1\pi^0$  interactions in the true 25 ton fiducial volume before the efficiency correction is applied. The systematic error in the fiducial volume correction is about 2% as shown in Table II-(B), which is estimated from the difference in the reconstructed vertex distribution of single  $\pi^0$  events for 1kt data and the neutrino Monte Carlo simulation.

Finally, the number of  $\text{NC}1\pi^0$  interactions in the true 25 ton fiducial volume is corrected for the detection efficiency in a bin by bin manner. Figure 3-(b) shows the detection efficiency for  $\text{NC}1\pi^0$  interactions as a function of real  $\pi^0$  momentum. The inefficiency for higher momentum  $\pi^0$ s is primarily due to reconstruction of only one ring for the  $\pi^0$  decay with highly asymmetric energies or small opening angle of two  $\gamma$ -rays. The overall detection efficiency for  $\text{NC}1\pi^0$  interactions, estimated by the neutrino Monte Carlo simulation, is 47% as shown in Table I. The systematic errors from the efficiency correction are due to uncertainties of reconstruction algorithms such as ring counting, particle identification and energy scale as listed in Table II-(C).

By a series of corrections for the background subtraction, the true/reconstruction fiducial difference and the detection efficiency, the true number of  $\text{NC}1\pi^0$  interactions in our data is measured to be  $(3.61 \pm 0.07 \pm 0.36) \times 10^3$  in the 25 ton fiducial volume. Figure 4 shows the measured momentum distribution of  $\text{NC}1\pi^0$  after all corrections, compared with the distribution predicted by the neutrino Monte Carlo simulation. The Monte Carlo histogram is normalized by the number of total neutrino events in the fiducial volume, which are selected by cuts

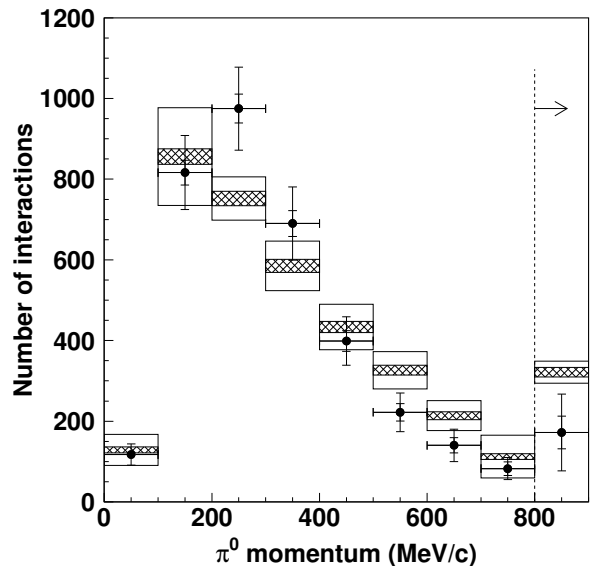


FIG. 4: The momentum distribution of  $\text{NC}1\pi^0$  events in the 25 ton fiducial volume (black dots). The inner and outer error bars attached to data points show statistical errors and total errors including systematic errors, respectively. The distribution predicted by the neutrino Monte Carlo simulation is also shown as a box histogram for comparison. The size of inner boxes represents Monte Carlo statistical errors. The size of outer boxes represents the uncertainty of the distribution shape due to neutrino interaction model ambiguity.

(i) to (v) as previously described. The size of outer boxes for the Monte Carlo histogram represents the uncertainty of the distribution shape of  $\text{NC}1\pi^0$  momentum

due to neutrino interaction model ambiguity, where the largest source is nuclear effects for pions in  $^{16}\text{O}$ . The measured distribution is in reasonably good agreement on the Monte Carlo estimation.

As previously described, we use CC interactions for normalization in order to derive the relative cross section for  $\text{NC}1\pi^0$  interactions. To make a CC enriched sample, FC  $\mu$ -like events and PC events are selected from the 1kt data during the same period. By using the CC enriched sample as a normalization, the uncertainty of the neutrino energy spectrum [5] is almost canceled in the measurement since the expected mean energy of neutrinos producing the CC sample, 1.45 GeV, is almost same as that of neutrinos producing the  $\pi^0$  sample, 1.50 GeV. The sample consists of 22,612 FC single-ring  $\mu$ -like events, 12,386 FC multi-ring events with the most energetic ring identified as  $\mu$ -like and 15,228 PC events, resulting in a total of 50,226 events. The  $\nu_\mu\text{CC}$  fraction in this sample is estimated to be 96 % by the neutrino Monte Carlo simulation (96.5 % for the FC single-ring  $\mu$ -like sample, 91.2 % for the FC multi-ring  $\mu$ -like sample and 98.5 % for the PC sample). The rest 4 % of the sample is mostly composed of NC interactions accompanying an outgoing charged pion above its Cherenkov threshold. The fiducial volume correction factor is estimated to be 1.02. The detection efficiency for  $\nu_\mu\text{CC}$  interactions by this selection is estimated to be 85%. The inefficiency mainly comes from mis-identification of the ring type in multi-ring events and  $\sim 100\text{ MeV}$  visible energy threshold by peak counting of the PMTSUM signal.

By applying non- $\nu_\mu\text{CC}$  background subtraction, fiducial volume correction and detection efficiency correction, the number of  $\nu_\mu\text{CC}$  neutrino interactions during the analysis period is measured to be  $(5.65 \pm 0.03 \pm 0.26) \times 10^4$  in the 25 ton fiducial volume. The estimated systematic errors are 4 % from the uncertainty of vertex reconstruction,

1 % from the uncertainty of neutrino interaction models, 1 % from the uncertainty of particle identification and 1 % from the uncertainty of absolute energy scale.

By taking the ratio, the relative cross section for  $\text{NC}1\pi^0$  interactions to the total  $\nu_\mu\text{CC}$  cross section is measured to be  $0.064 \pm 0.001(\text{stat.}) \pm 0.007(\text{sys.})$ . Our neutrino interaction models predict the ratio to be 0.065, which results in good agreement. For reference, the total  $\nu_\mu\text{CC}$  cross section is calculated to be  $1.1 \times 10^{-38} \text{ cm}^2/\text{nucleon}$  in the neutrino Monte Carlo simulation by averaging over the K2K neutrino beam energy.

In summary, we have measured the rate and the  $\pi^0$  momentum distribution of NC single  $\pi^0$  production by neutrinos with a mean energy of 1.3 GeV at the K2K 1kt water Cherenkov detector. The cross section ratio to total  $\nu_\mu\text{CC}$  neutrino interaction is obtained as  $0.064 \pm 0.001(\text{stat.}) \pm 0.007(\text{sys.})$ , showing good agreement with the prediction by our neutrino interaction models. This measurement provides essential information for an understanding of  $\pi^0$  production in water at the 1 GeV neutrino energy region, which is relevant for present and future neutrino oscillation experiments.

We thank the KEK and ICRR Directorates for their strong support and encouragement. K2K is made possible by the inventiveness and the diligent efforts of the KEK-PS machine and beam channel groups. We gratefully acknowledge the cooperation of the Kamioka Mining and Smelting Company. This work has been supported by the Ministry of Education, Culture, Sports, Science and Technology, Government of Japan and its grants for Scientific Research, the Japan Society for Promotion of Science, the U.S. Department of Energy, the Korea Research Foundation, the Korea Science and Engineering Foundation, the CHEP in Korea, and Polish KBN grant 1P03B03826 and 1P03B08227.

- 
- [1] Y. Fukuda et al. (Super-Kamiokande), Phys. Rev. Lett. **81**, 1562 (1998), hep-ex/9807003.
  - [2] M. H. Ahn et al. (K2K), Phys. Rev. Lett. (2004), to be published, hep-ex/0402017.
  - [3] S. H. Ahn et al. (K2K), Phys. Lett. **B511**, 178 (2001), hep-ex/0103001.
  - [4] Y. Itow et al. (2001), hep-ex/0106019, URL <http://neutrino.kek.jp/jhfnu/>.
  - [5] M. H. Ahn et al. (K2K), Phys. Rev. Lett. **90**, 041801 (2003), hep-ex/0212007.
  - [6] Y. Fukuda et al., Nucl. Instrum. Meth. **A501**, 418 (2003).
  - [7] Y. Fukuda et al. (Super-Kamiokande), Phys. Lett. **B433**, 9 (1998), hep-ex/9803006.
  - [8] M. Shiozawa (Super-Kamiokande), Nucl. Instrum. Meth. **A433**, 240 (1999).
  - [9] Y. Hayato, Nucl. Phys. Proc. Suppl. **112**, 171 (2002).
  - [10] C. H. Llewellyn Smith, Phys. Rept. **3**, 261 (1972).
  - [11] D. Rein and L. M. Sehgal, Ann. Phys. **133**, 79 (1981).
  - [12] S. K. Singh, M. J. Vicente-Vacas, and E. Oset, Phys. Lett. **B416**, 23 (1998).
  - [13] D. Rein and L. M. Sehgal, Nucl. Phys. **B223**, 29 (1983).
  - [14] J. Marteau, J. Delorme, and M. Ericson, Nucl. Instrum. Meth. **A451**, 76 (2000).
  - [15] M. Gluck, E. Reya, and A. Vogt, Z. Phys. **C67**, 433 (1995).
  - [16] A. Bodek and U. K. Yang, Nucl. Phys. Proc. Suppl. **112**, 70 (2002), hep-ex/0203009.
  - [17] T. Sjostrand, Comput. Phys. Commun. **82**, 74 (1994).
  - [18] M. Nakahata et al. (KAMIOKANDE), J. Phys. Soc. Jap. **55**, 3786 (1986).
  - [19] R. D. Woods and D. S. Saxon, Phys. Rev. **95**, 577 (1954).
  - [20] L. L. Salcedo, E. Oset, M. J. Vicente-Vacas, and C. Garcia-Recio, Nucl. Phys. **A484**, 557 (1988).
  - [21] G. Rowe, M. Salomon, and R. H. Landau, Phys. Rev. **C18**, 584 (1978).
  - [22] H. Ejiri, Phys. Rev. **C48**, 1442 (1993).